

Investigating the Temporal Evolution of Gamma-Ray Burst Central Engine Parameters Based on Numerical Simulations

Wei-Hua Lei

Department of Astronomy, School of Physics, Huazhong University of Science and Technology, Wuhan, 430074, China

arXiv:2603.15028v1 [astro-ph.HE] 16 Mar 2026

Abstract

A hyperaccreting stellar-mass black hole (BH) has been proposed as the candidate central engine of gamma-ray bursts (GRBs). Comparing the predictions from the central engine models with the temporal behavior of GRBs is of great interest. In this paper, using the open-source GRMHD HARM-COOL code, we evolve several 2D magnetized hyperaccreting BH models with realistic equation of state in a fixed curved space-time background. We extend the code to include the calculation of neutrino annihilation power. We then study the time evolution of BH central engine parameters, i.e., the neutrino annihilation power, the Blandford-Znajek (BZ) power, and the initial magnetization σ_0 . We find that the neutrino power is generally consistent with previous analytical results. Usually, the neutrino annihilation process tends to launch a thermal “fireball”, while the BZ jet is Poynting-flux-dominated. Our results, especially the evolution characteristics of σ_0 may help to understand the complex GRB spectral behavior.

Keywords:

gamma-ray bursts, black hole, accretion disk

1. Introduction

Rich observations have greatly enhanced our knowledge of gamma-ray bursts (GRBs). The association between long GRBs and Type Ic supernovae suggests their origin of massive star core-collapse (Woosley, 1993; Paczyński, 1998; MacFadyen and Woosley, 1999), and the occurrence of GW170817 accompanied by GRB 170817A (Abbott et al., 2017; Kasliwal et al., 2017) supports the binary merger (neutron star-neutron star, or neutron star-black hole) origin model of short GRBs invoking mergers of two neutron stars (NSs) or of a black hole (BH) and an NS (Eichler et al., 1989; Paczynski, 1991; Fryer et al., 1999). However, the nature and property of GRB central engines are still poorly understood.

The popular GRB central engine model invokes a stellar-mass BH surrounded by a hyperaccretion disk (the so-called neutrino-cooling-dominated accretion flow, NDAF). The relativistic jet in a GRB can be powered by the neutrino-antineutrino annihilation mechanism (Popham et al., 1999; Di Matteo et al., 2002; Gu et al., 2006; Chen and Beloborodov, 2007; Janiuk et al., 2007;

Lei et al., 2009; Cao et al., 2014; Xie et al., 2016; Liu et al., 2007, 2017), or the Blandford-Znajek (Blandford and Znajek, 1977, hereafter BZ) mechanism (Lee et al., 2000; Li and Paczyński, 2000; Lei et al., 2005; Lei and Zhang, 2011; Lei et al., 2013, 2017; Liu, 2018). It is crucial to differentiate these different mechanisms using observational data.

The temporal behavior of GRBs in the prompt emission phase may provide meaningful clues to the central engine models. In some GRBs (e.g., GRB 080916C), the spectra studies show no evidence of quasi-thermal emission. This motivates us to investigate the evolution of the BH central engine and compare their predictions with the temporal behavior of GRBs.

In our previous work, we addressed the fundamental problem of baryon loading in GRB jets, and found that a magnetically dominated jet can be much cleaner and is more consistent with the requirement of large Lorentz factors in GRBs (Lei et al., 2013). We then investigated the BH central engine parameters, such as the jet power, the dimensionless entropy η , and the central engine parameter $\mu_0 = \eta(1 + \sigma_0)$ (where σ_0 is the initial magnetization of the engine) at the base of the jet (Lei et al., 2017). With these results, a number of works adopted some empirical

Email address: leiwh@hust.edu.cn (Wei-Hua Lei)

¹Preprint submitted to Journal of High Energy Astrophysics

correlations (such as jet power vs. Lorentz factor Γ_0 and minimum variability timescale vs. the Lorentz factor Γ_0) (Xie et al., 2017; Yi et al., 2017, 2021; Lloyd-Ronning et al., 2018; Li et al., 2018), or the spectral evolution characteristics of prompt emissions (Gao et al., 2022; Zhang et al., 2024; Fu et al., 2024), to differentiate the central engine models. However, these studies are mainly based on analytical solutions to the NADF and BZ models.

The general relativistic magnetohydrodynamic (GRMHD) code HARM (High Accuracy Magnetohydrodynamics) is a finite-volume code with HLL shock capturing scheme, which works on the stationary metric around the BH. The code integrates the total energy equation and updates the set of “conserved” variable, i.e., comoving density, energy-momentum, and magnetic field (Gammie et al., 2003). Janiuk (2017) self-consistently incorporated the detailed nuclear equation of state (the degeneracy of relativistic electrons, protons, and neutrons) into the HARM scheme (Janiuk et al., 2007; Janiuk, 2017, 2019). With this developed code, namely HARM-COOL, they investigated the temporal evolution of the neutrino flux, the BZ power and r-process nucleosynthesis in the outflow (Janiuk, 2017, 2019; Sapountzis and Janiuk, 2019). However, the estimation of the neutrino annihilation power, which is fundamental in the study of the central engine of GRBs, is lacking in the code.

In this paper, we perform 2D GRMHD simulations for the hyperaccreting BH with HARM-COOL, and include the treatment of neutrino annihilation. We then investigate the evolution of the central engine parameters, such as the jet power and the initial magnetization.

This paper is organized as follows. In Section 2, we present the simulation scheme and the initial configuration of the HARM-COOL. The calculation of neutrino annihilation luminosity, BZ power and magnetization parameter σ_0 are given in Sections 2 and 3. Finally, we summarize our results and discuss some related issues in Section 4.

2. The Simulation Setup

The GRMHD code HARM provides a solver for continuity and energy-momentum conservation equations (Gammie et al., 2003; Noble et al., 2006)

$$\begin{aligned}(\rho u^\mu)_{;\mu} &= 0, \\ T_{\nu;\mu}^\mu &= 0,\end{aligned}\quad (1)$$

and induction equation,

$$\partial_i(\sqrt{-g}B^i) = -\partial_j[\sqrt{-g}(b^j u^i - b^i u^j)].\quad (2)$$

The conservative numerical scheme used in this code solves $\partial_t \mathbf{U}(\mathbf{P}) = -\partial_i \mathbf{F}^i(\mathbf{P}) + \mathbf{S}(\mathbf{P})$, where \mathbf{U} is a vector of “conserved” variables (momentum, energy density, number density, taken in the coordinate frame), \mathbf{P} is a vector of “primitive” variables (rest-mass density, internal energy), \mathbf{F}^i are the fluxes, and \mathbf{S} is a vector of source terms. Inversion $\mathbf{P}(\mathbf{U})$ is calculated, therefore, in every time step, numerically.

In HARM-COOL, the nuclear equation of state is incorporated into the code (Janiuk, 2017, 2019). The total pressure is contributed by free nucleons, pairs, radiation, alpha particles, and also trapped neutrinos (Yuan, 2005; Janiuk et al., 2007), and is given by:

$$P_{\text{gas}} = P_{\text{nucl}} + P_{\text{He}} + P_{\text{rad}} + P_{\nu},\quad (3)$$

where $P_{\text{nucl}} = P_{e^-} + P_{e^+} + P_n + P_p$ and

$$P_i = \frac{2\sqrt{2}}{3\pi^2} \frac{(m_i c^2)^4}{(\hbar c)^3} \beta_i^{5/2} [F_{3/2}(\eta_i, \beta_i) + \frac{1}{2} \beta_i F_{5/2}(\eta_i, \beta_i)],\quad (4)$$

where F_k are the Fermi-Dirac integrals of the order k , η_i are the reduced chemical potentials, and $\beta_i = kT/m_i c^2$ are the relativity parameters. The pressure of helium is taken as ideal gas, $P_{\text{He}} = (n_b/4)(1 - X_{\text{nuc}})kT$. The radiation pressure, $P_{\text{rad}} = (4\sigma)/(3c)T^4$.

The expression for neutrino cooling rate Q_ν is (Di Matteo et al., 2002)

$$Q_\nu = \sum \frac{(7/8)\sigma T^4}{(3/4)(\tau_{\nu_i}/2 + 1/\sqrt{3} + 1/(3\tau_{a,\nu_i}))},\quad (5)$$

where $\tau_i = \tau_{a,i} + \tau_s$, $\tau_{a,i}$ and τ_s denote absorption and scattering.

The detailed discussions over nuclear equation of state and neutrino treatment implemented in HARM-COOL code are given in (Janiuk et al., 2013) and (Janiuk, 2017, 2019).

The initial conditions for the accreting material is modeled as an equilibrium torus solution, defined as in Fishbone and Moncrief (1976, FM). The FM disk is defined by r_{in} the inner radius of the disk, r_{max} the radius of maximum pressure, and a dimensionless BH spin a_\bullet .

The BH mass has been set to be $M_\bullet = 3M_\odot$ in our simulations. We conveniently adopt the scaling factor, r_{in} and r_{max} , so that the FM torus mass of $M_{\text{torus}} \sim 0.1M_\odot$. We seed the torus with a poloidal magnetic field (magnetic field lines follow the constant density surfaces); the strength of the initial magnetic field is normalized by the gas to a magnetic pressure ratio at the pressure maximum of the initial structure of the disk ($\beta \equiv p_{\text{gas}}/p_{\text{mag}} = 50$). We examine three sets of models with different differing with the BH spin ($a_\bullet = 0.1, 0.6, 0.9, 0.98$). Table 1

presents a summary of the models and their initial parameters. Our grid resolution is 128×128 .

In Fig. 1, we plot the accretion rate as the function of time. The instantaneous peaks, which appear in the states of a highly variable accretion rate, reach the values up to several solar masses per second.

3. Neutrino Annihilation Power

The HARM-COOL code provides the calculation for the total neutrino luminosity, but does not include the estimation for the neutrino annihilation luminosity (Janiuk, 2017, 2019). The later is, however, more important for a direct comparison with the observations.

From the HARM-COOL simulations, we can get the neutrino mean energy $\epsilon_{\nu_i}^k$ and luminosity $l_{\nu_i}^k$ in each grid cell k . The angle at which neutrinos from cell k encounter anti-neutrinos from another cell k' at that point is denoted as $\theta_{kk'}$. The height (neutrino annihilation occurs) above (or below) the disk equatorial plane is d_k . We write a code to incorporate the neutrino annihilation luminosity by summing over all pairs of cells (Popham et al., 1999; Rosswog et al., 2003),

$$\begin{aligned} \dot{E}_{\nu\bar{\nu}} = & A_1 \sum_k \frac{l_{\nu_i}^k}{d_k^2} \sum_{k'} \frac{l_{\nu_i}^{k'}}{d_{k'}^2} (\epsilon_{\nu_i}^k + \epsilon_{\nu_i}^{k'}) (1 - \cos \theta_{kk'})^2 + \\ & A_2 \sum_k \frac{l_{\nu_i}^k}{d_k^2} \sum_{k'} \frac{l_{\nu_i}^{k'}}{d_{k'}^2} \frac{\epsilon_{\nu_i}^k + \epsilon_{\nu_i}^{k'}}{\epsilon_{\nu_i}^k \epsilon_{\nu_i}^{k'}} (1 - \cos \theta_{kk'}), \end{aligned} \quad (6)$$

where $A_1 \approx 1.7 \times 10^{-44} \text{ cm} \cdot \text{erg}^{-2} \cdot \text{s}^{-1}$ and $A_2 \approx 1.6 \times 10^{-56} \text{ cm} \cdot \text{erg}^{-2} \text{s}^{-1}$. The summation is performed over the whole space outside the BH horizon and the disk. The disk height H is given by (Janiuk, 2017),

$$H = \frac{c}{\Omega_D} \sqrt{\frac{P}{\rho c^2 + e}}, \quad (7)$$

where $\Omega_D = \frac{c^3}{GM_\bullet} \frac{1}{a_\bullet + (r/r_g)^{3/2}}$ is the Keplerian frequency.

The neutrino annihilation power as a function of time is shown in Fig. 2. We present the results for different BH spins, i.e., $a_\bullet = 0.1$ (top left), 0.6 (top right), 0.9 (bottom left) and 0.98 (bottom right), see the solid red lines. We also plot the total neutrino power with solid green lines. Inspecting Fig. 2, both the neutrino annihilation power $\dot{E}_{\nu\bar{\nu}}$ and the neutrino power \dot{E}_ν on average are scaling with the BH spin.

For comparison, we calculate the neutrino annihilation

power from the analytical solutions, i.e., (Lei et al., 2017)

$$\begin{aligned} \dot{E}_{\nu\bar{\nu}}^{\text{LZWL}} \simeq & \dot{E}_{\nu\bar{\nu},\text{ign}} \left[\left(\frac{\dot{m}}{\dot{m}_{\text{ign}}} \right)^{-\alpha_{\nu\bar{\nu}}} + \left(\frac{\dot{m}}{\dot{m}_{\text{ign}}} \right)^{-\beta_{\nu\bar{\nu}}} \right]^{-1} \\ & \times \left[1 + \left(\frac{\dot{m}}{\dot{m}_{\text{trap}}} \right)^{\beta_{\nu\bar{\nu}} - \gamma_{\nu\bar{\nu}}} \right]^{-1}, \end{aligned} \quad (8)$$

where,

$$\begin{cases} \dot{E}_{\nu\bar{\nu},\text{ign}} = 10^{(48.0+0.15a_\bullet)} \left(\frac{m_\bullet}{3} \right)^{\log(\dot{m}/\dot{m}_{\text{ign}}) - 3.3} \text{ erg s}^{-1}, \\ \alpha_{\nu\bar{\nu}} = 4.7, \beta_{\nu\bar{\nu}} = 2.23, \gamma_{\nu\bar{\nu}} = 0.3, \\ \dot{m}_{\text{ign}} = 0.07 - 0.063a_\bullet, \dot{m}_{\text{trap}} = 6.0 - 4.0a_\bullet^3, \end{cases} \quad (9)$$

where $m_\bullet = M_\bullet/M_\odot$, and $\dot{m} = \dot{M}/M_\odot \text{s}^{-1}$. \dot{m}_{ign} and \dot{m}_{trap} are the igniting and trapping accretion rates, respectively. We adopt $m_\bullet = 3$, and use the accretion rate \dot{m} from the simulations (see Fig. 1) for different models, i.e., Mt0.1-a0.1 (top left), Mt0.1-a0.6 (top right), Mt0.1-a0.9 (bottom left) and Mt0.11-a0.98 (bottom right), as shown with dashed gray lines in Fig. 2. As we can see that the $\dot{E}_{\nu\bar{\nu}}$ obtained based on HARM-COOL is roughly consistent with our previous analytical result (Lei et al., 2017).

4. Magnetic Power

Utilizing the magnetic flux Φ_{BH} through the BH horizon from HARM-COOL simulations, one can estimate the BZ power.

The BZ jet power from a BH with mass M_\bullet and angular momentum J_\bullet is (Lee et al., 2000; Li and Paczyński, 2000; Wang et al., 2002; McKinney, 2005; Lei et al., 2005; Lei and Zhang, 2011; Lei et al., 2013)

$$\dot{E}_B = \frac{c}{64\pi^2} \Phi_{\text{BH}}^2 q^2 F(a_\bullet), \quad (10)$$

where $F(a_\bullet) = [(1+q^2)/q^2][(q+1/q)\arctan q - 1]$, and $q = a_\bullet/(1+\sqrt{1-a_\bullet^2})$. The evolution of BZ power for different models is plotted in Fig. 3 with blue lines.

For comparison, we also plot the other expressions. Blandford and Znajek (1977) showed that magnetic power of a force-free jet from a slowly spinning BH ($a_\bullet \ll 1$) is (Blandford and Znajek, 1977; Barkov and Baushev, 2011)

$$\dot{E}_B^{\text{BZ77}} = \frac{\kappa c}{4\pi} \Phi_{\text{BH}}^2 \frac{a_\bullet^2}{16r_g^2}, \quad (11)$$

where κ depends weakly on the field geometry (it is 0.053 for a split monopole geometry and 0.044 for a parabolic geometry), Φ_{BH} is an absolute magnetic flux through the BH. The results for \dot{E}_B^{BZ77} are shown with dotted blue lines in Fig. 3.

Table 1: Setup of the Models

Model	a_\bullet	β_0	$M_\bullet(M_\odot)$	$M_t(M_\odot)$	$r_{\text{in}}(r_g)$	$r_{\text{max}}(r_g)$
Mt0.1-a0.1	0.1	50	3	0.1	7.0	14.1
Mt0.1-a0.6	0.6	50	3	0.1	6.0	12.2
Mt0.1-a0.9	0.9	50	3	0.1	5.0	10.7
Mt0.11-a0.98	0.98	50	3	0.11	3.1	9.1

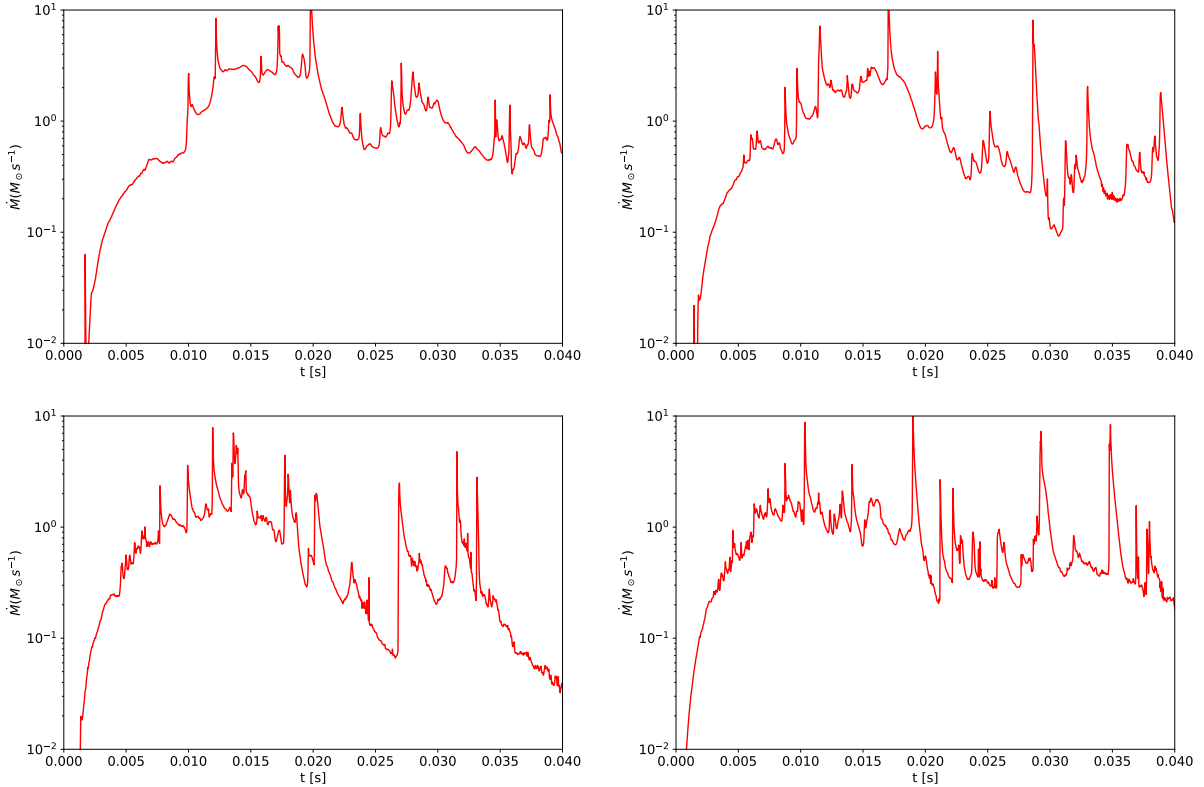


Figure 1: The time evolution of the accretion rate for the system with BH mass of $M_{\text{bh}} = 3M_\odot$ and the initial disk mass of $M_t = 0.1M_\odot$. We consider four cases: $a_\bullet = 0.1$ (top left), $a_\bullet = 0.6$ (top right), 0.9 (bottom left) and 0.98 (bottom right).

Tchekhovskoy et al. (2010) extended the magnetic power in Blandford and Znajek (1977) to high-spin BHs and obtained (Tchekhovskoy et al., 2010; Tchekhovskoy and McKinney, 2012)

$$\dot{E}_B^{\text{TNM}} = \frac{\kappa}{4\pi c} \Phi_{\text{BH}}^2 \Omega_\bullet^2 f(\Omega_\bullet), \quad (12)$$

where $f(\Omega_\bullet) \simeq 1 + 1.38(\Omega_\bullet r_g/c)^2 - 9.2(\Omega_\bullet r_g/c)^4$ is a high-spin correction to Eq.(11). The results for \dot{E}_B^{TNM} are shown with dashed blue lines in Fig.3.

We present the results for different BH spins, i.e., $a_\bullet = 0.1$ (top left), $a_\bullet = 0.6$ (top right), 0.9 (bottom left) and 0.98 (bottom right). The power of BZ \dot{E}_B with the formula of Eq. (10) is found to be quite close to \dot{E}_B^{TNM} in all cases. However, the expression \dot{E}_B^{BZ77} can only apply to the case

with low BH spin. In high BH spin case (like $a_\bullet = 0.98$), \dot{E}_B^{BZ77} is significantly smaller than \dot{E}_B . For $a_\bullet = 0.1$, the difference between their values (\dot{E}_B , \dot{E}_B^{BZ77} and \dot{E}_B^{TNM}) is nearly indistinguishable.

For comparison, we also show the evolution of the neutrino annihilation power $\dot{E}_{\nu\bar{\nu}}$ in Fig. 3 (see the red lines). The neutrino annihilation power is always dominated at the beginning, since the magnetic flux is still building. The BZ luminosity gradually becomes dominant during the evolution for high spin BH. For $a_\bullet = 0.1$, the jet luminosity is dominated by $\dot{E}_{\nu\bar{\nu}}$ for some time intervals, while by \dot{E}_B in other episodes, see the top left panel of Fig. 3.

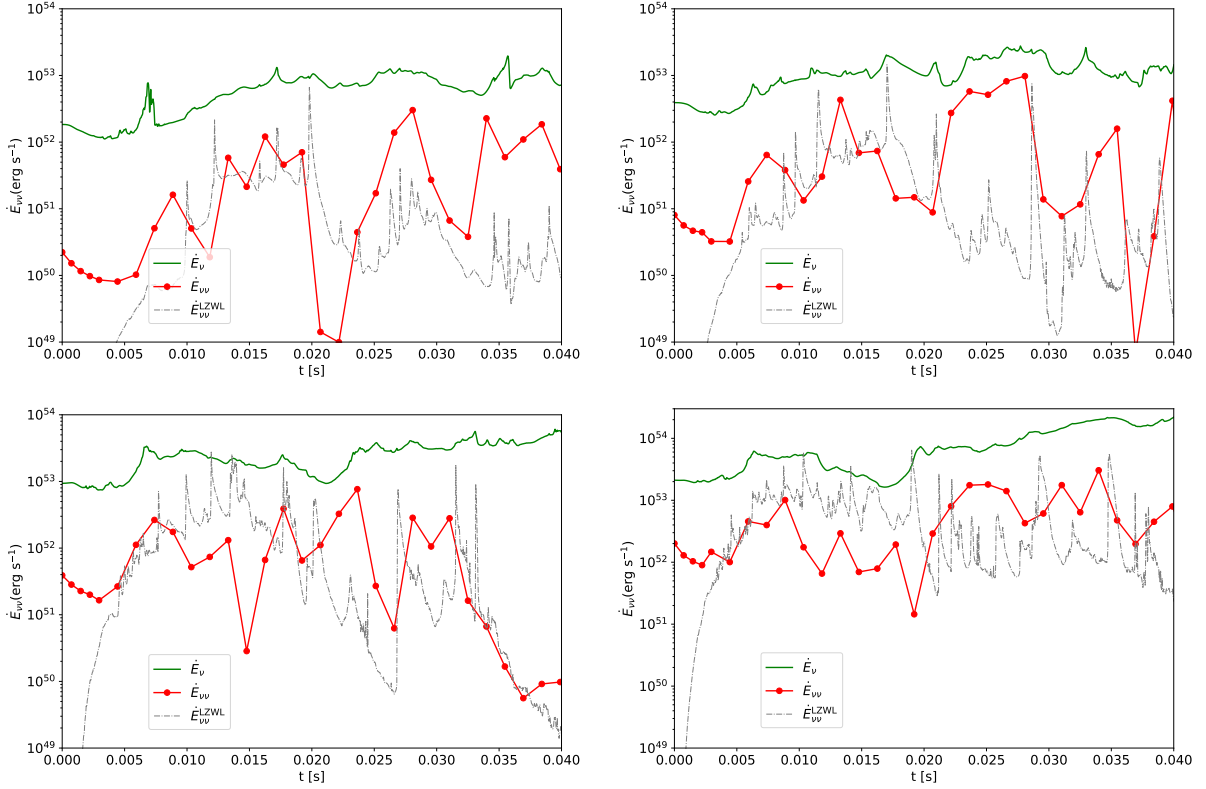


Figure 2: The time evolution of the neutrino annihilation power for a BH with mass $m_{\bullet} = 3$, and spin $a_{\bullet} = 0.1$ (top left), $a_{\bullet} = 0.6$ (top right), 0.9 (bottom left) and 0.98 (bottom right).

We can define the magnetization parameter,

$$\sigma_0 = \frac{\dot{E}_{\text{BZ}}}{\dot{E}_{\text{m}}}, \quad (13)$$

where $\dot{E}_{\text{m}} = \dot{E}_{\nu\bar{\nu}} + \dot{M}_{\text{j}}c^2$, and \dot{M}_{j} is the baryon loading rate for GRB jet (Lei et al., 2013, 2017). In GRB prompt emission phase, $\dot{E}_{\nu\bar{\nu}}$ is usually much larger than $\dot{M}_{\text{j}}c^2$, leading to an extreme relativistic jet. Therefore, we take $\sigma_0 \sim \dot{E}_{\text{B}}/\dot{E}_{\nu\bar{\nu}}$. The time evolution of σ_0 is presented in Fig.4 for Mt0.1-a0.1 (black lines), Mt0.1-a0.6 (red lines), Mt0.1-a0.9 (green lines) and Mt0.11-a0.98 (blue lines) models. For comparison, σ_0 calculated with \dot{E}_{B} , $\dot{E}_{\text{B}}^{\text{BZ77}}$ and $\dot{E}_{\text{B}}^{\text{TNM}}$ are also presented with solid, dotted, and dashed lines, respectively. We find a highly variable σ_0 . On average, $\sigma_0 \sim 1$ for $a_{\bullet} = 0.1$, while $\sigma_0 > 1$ for high spin cases.

5. Discussions

The central engine of GRBs is likely a hyperaccreting BH. The neutrino annihilation and BZ processes are two candidate mechanisms for powering GRB jets. In this paper, we extended the HARM-COOL code to include the

calculation of neutrino annihilation power, and studied the time evolution of the central engine parameters for these two models.

The evolution of $\dot{E}_{\nu\bar{\nu}}$, \dot{E}_{B} and σ_0 exhibits high variability. The $\dot{E}_{\nu\bar{\nu}}$ obtained based on HARM-COOL is roughly consistent with our previous analytical result (Lei et al., 2017). We also find that the neutrino-annihilation power $\dot{E}_{\nu\bar{\nu}}$ increases with BH spin. The BZ power is calculated by using the magnetic flux from the code and with three different analytical expressions. The difference of \dot{E}_{B} with the different expressions is significant for high spin BH and can be ignored for very low spin case.

As discussed in Lei et al. (2013, 2017), the neutrino annihilation mechanism launches a thermal “fireball”, leaving an imprint of the thermal component in the GRB spectrum. However, a jet powered by the BZ mechanism is Poynting-flux-dominated. In this paper, we find that the neutrino annihilation power is dominated at the beginning, and the BZ luminosity gradually becomes dominant during the evolution for high spin BH. For very low spin case, like $a_{\bullet} = 0.1$, the jet luminosity is dominated by $\dot{E}_{\nu\bar{\nu}}$ for some time intervals, while by \dot{E}_{B} in other episodes. The prompt emission of GRB 200613A show a signifi-

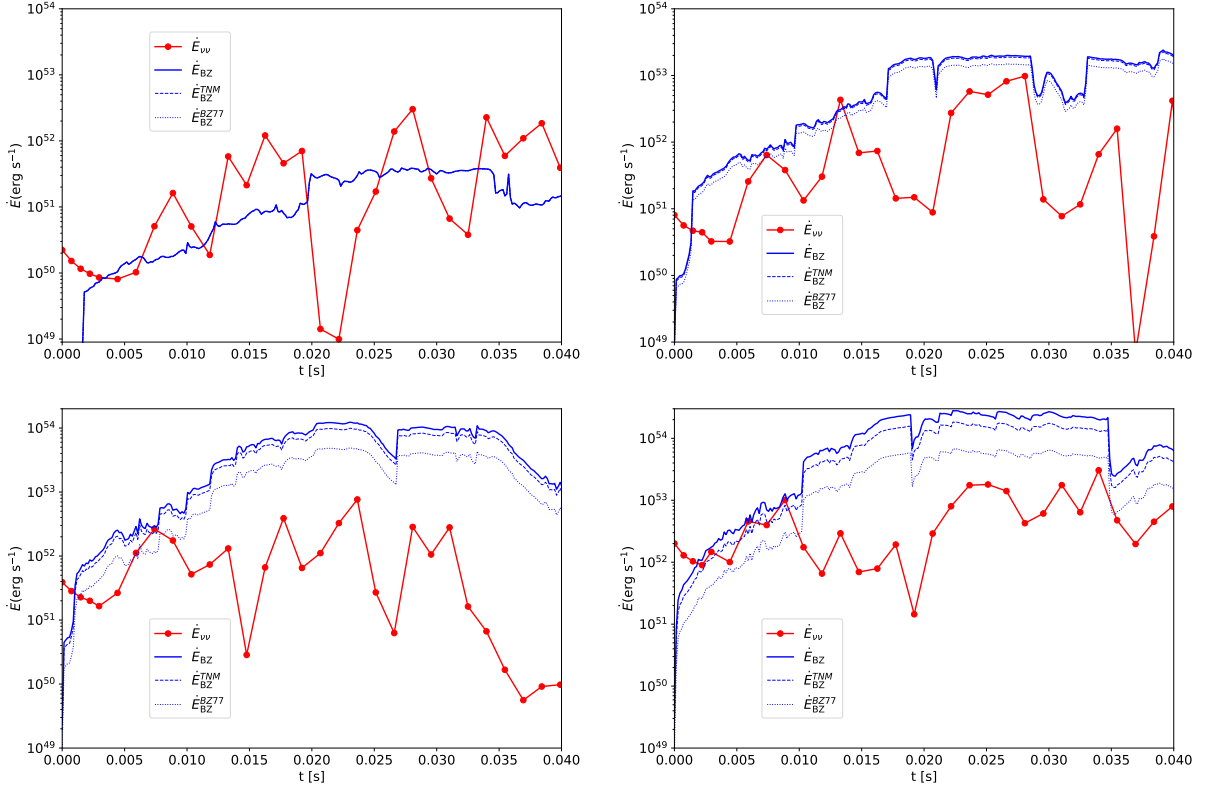


Figure 3: The time evolution of the BZ power \dot{E}_B (solid blue lines) for a BH with mass $m_* = 3$, and spin $a_* = 0.1$ (top left), $a_* = 0.6$ (top right), 0.9 (bottom left) and 0.98 (bottom right). For comparisons, we also show the results of \dot{E}_B^{BZ77} (dotted blue lines), \dot{E}_B^{TNM} (dashed blue lines), and the neutrino power $\dot{E}_{\nu\bar{\nu}}$ (red lines).

cant spectral evolution from a fireball to a Pyontying-flux-dominated jet (Zhang et al., 2018), which might be interpreted with the building-up of magnetic flux or spin-up of the central BH. Recently, Fu et al. (2024) performed a time-resolved spectral analysis of the prompt emission of GRB 200613A, and revealed that the BB components are only significant in some time intervals and do not appear in other time periods. Such evolution behavior of prompt spectra could be understood with our simulation results by relating the BB component to the neutrino annihilation power and the Band component to the BZ power. As to σ_0 , Gao and Zhang (2015) also found the variation of the magnetic parameter during the prompt phase of GRB 110721A.

The baryon loading is another fundamental parameter of GRB, we derived the baryon loading rate and the evolution based on analytical solutions in previous works (Lei et al., 2013, 2017). In this paper, we ignore the baryon loading. Sapountzis and Janiuk (2019) pointed out that the formation of a magnetic barrier leads to the launch of a low baryon jet and estimated the maximum achievable Lorentz factor in the jets produced by simulations (Janiuk et al., 2021). However, they mainly focused on the purely

electromagnetic effects and ignored the potential neutrino implications on the launching process. Our estimation of neutrino annihilation power will remain a good extension for this problem.

In this paper, we conduct the simulation in a fixed background metric. Instead of using a stationary metric with the BH having constant mass and spin and simply allowing the matter to accrete onto it, Janiuk et al. (2018) extend the code to account for a changing Kerr metric. This will be included in future work.

GRBs are also expected to occur in dense environments, e.g., the accretion disk of active galactic nuclei (AGN) (Zhu et al., 2021; Perna et al., 2021; Yuan et al., 2022; Yuan and Lei, 2025). Kathirgamaraju et al. (2024) performed GRMHD simulations (with HARM) of a binary neutron star mergers occurring within AGN disks, and studied the jet launch and observability of GRB afterglow. We can also include the neutrino process in these studies.

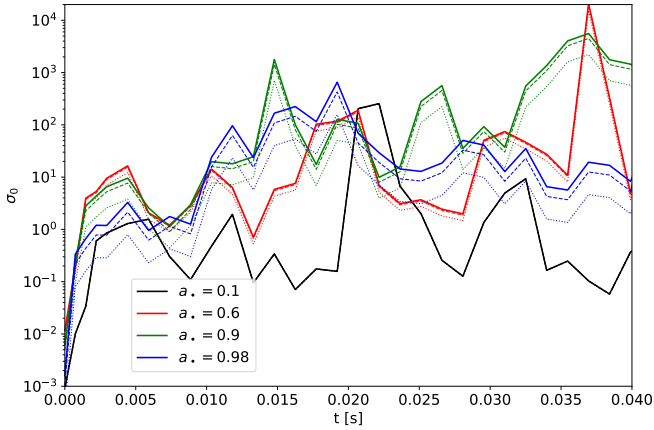


Figure 4: The time evolution of the magnetization parameter σ_0 for a BH with mass $m_* = 3$, and spin $a_* = 0.1$ (black), $a_* = 0.6$ (red), $a_* = 0.9$ (green), and $a_* = 0.98$ (blue). The solid, dotted and dashed lines represent σ_0 calculated with \dot{E}_B , \dot{E}_B^{BZ77} and \dot{E}_B^{TNM} , respectively.

Acknowledgements

We are very grateful to Agnieszka Janiuk, He Gao and Bing Zhang for their helpful discussions. This work is supported by the National Natural Science Foundation of China under grants 12473012 and 12533005, and the National Key R&D Program of China (No. SQ2023YFC220007).

References

Abbott, B.P., Abbott, R., Abbott, T.D., Acernese, F., Ackley, K., Adams, C., Adams, T., Addesso, P., Adhikari, R.X., Adya, V.B., Affeldt, C., Afrough, M., Agarwal, B., Agathos, M., Agatsuma, K., Aggarwal, N., Aguiar, O.D., Aiello, L., Ain, A., Ajith, P., Allen, B., Allen, G., Allocca, A., Altin, P.A., Amato, A., Ananyeva, A., Anderson, S.B., Anderson, W.G., Angelova, S.V., Antier, S., Appert, S., Arai, K., Araya, M.C., Areeda, J.S., Arnaud, N., Arun, K.G., Ascenzi, S., Ashton, G., Ast, M., Aston, S.M., Astone, P., Atallah, D.V., Aufmuth, P., Aulbert, C., AultONeal, K., Austin, C., Avila-Alvarez, A., Babak, S., Bacon, P., Bader, M.K.M., Bae, S., Bailes, M., Baker, P.T., Baldaccini, F., Ballardín, G., Ballmer, S.W., Banagiri, S., Barayoga, J.C., Barclay, S.E., Barish, B.C., Barker, D., Barkett, K., Barone, F., Barr, B., Barsotti, L., Barsuglia, M., Barta, D., Barthelmy, S.D., Bartlett, J., Bartos, I., Bassiri, R., Basti, A., Batch, J.C., Bawaj, M., Bayley, J.C., Bazzan, M., Bécsy, B., Beer, C., Bejger, M., Belahcene, I., Bell, A.S., Berger, B.K., Bergmann, G., Bernuzzi, S., Bero, J.J., Berry, C.P.L., Bersanetti,

D., Bertolini, A., Betzwieser, J., Bhagwat, S., Bhandare, R., Bilenko, I.A., Billingsley, G., Billman, C.R., Birch, J., Birney, R., Birnholtz, O., Biscans, S., Biscoveanu, S., Bisht, A., Bitossi, M., Biwer, C., Bizouard, M.A., Blackburn, J.K., Blackman, J., Blair, C.D., Blair, D.G., Blair, R.M., Bloemen, S., Bock, O., Bode, N., Boer, M., Bogaert, G., Bohe, A., Bondu, F., Bonilla, E., Bonnand, R., Boom, B.A., Bork, R., Boschi, V., Bose, S., Bossie, K., Bouffanais, Y., Bozzi, A., Bradaschia, C., Brady, P.R., Branchesi, M., Brau, J.E., Briant, T., Brillet, A., Brinkmann, M., Brisson, V., Brockill, P., Broida, J.E., Brooks, A.F., Brown, D.A., Brown, D.D., Brunett, S., Buchanan, C.C., Buikema, A., Bulik, T., Bulten, H.J., Buonanno, A., Buskulic, D., Buy, C., Byer, R.L., Cabero, M., Cadonati, L., Cagnoli, G., Cahillane, C., Calderón Bustillo, J., Callister, T.A., Calloni, E., Camp, J.B., Canepa, M., Canizares, P., Cannon, K.C., Cao, H., Cao, J., Capano, C.D., Capocasa, E., Carbognani, F., Caride, S., Carney, M.F., Carullo, G., Casanueva Diaz, J., Casentini, C., Caudill, S., Cavaglià, M., Cavalier, F., Cavalieri, R., Cella, G., Cepeda, C.B., Cerdá-Durán, P., Cerretani, G., Cesarini, E., Chamberlin, S.J., Chan, M., Chao, S., Charlton, P., Chase, E., Chassande-Mottin, E., Chatterjee, D., Chatziioannou, K., Cheeseboro, B.D., Chen, H.Y., Chen, X., Chen, Y., Cheng, H.P., Chia, H., Chincarini, A., Chiummo, A., Chmiel, T., Cho, H.S., Cho, M., Chow, J.H., Christensen, N., Chu, Q., Chua, A.J.K., Chua, S., 2017. GW170817: Observation of Gravitational Waves from a Binary Neutron Star Inspiral. *Phys. Rev. Lett.* 119, 161101. doi:[10.1103/PhysRevLett.119.161101](https://doi.org/10.1103/PhysRevLett.119.161101), [arXiv:1710.05832](https://arxiv.org/abs/1710.05832).

Barkov, M.V., Baushev, A.N., 2011. Accretion of a massive magnetized torus on a rotating black hole. *Nature Communications* 16, 46–56. doi:[10.1016/j.newast.2010.07.001](https://doi.org/10.1016/j.newast.2010.07.001), [arXiv:0905.4440](https://arxiv.org/abs/0905.4440).

Blandford, R.D., Znajek, R.L., 1977. Electromagnetic extraction of energy from Kerr black holes. *MNRAS* 179, 433–456. doi:[10.1093/mnras/179.3.433](https://doi.org/10.1093/mnras/179.3.433).

Cao, X., Liang, E.W., Yuan, Y.F., 2014. Episodic Jet Power Extracted from a Spinning Black Hole Surrounded by a Neutrino-dominated Accretion Flow in Gamma-Ray Bursts. *ApJ* 789, 129. doi:[10.1088/0004-637X/789/2/129](https://doi.org/10.1088/0004-637X/789/2/129), [arXiv:1405.7097](https://arxiv.org/abs/1405.7097).

Chen, W.X., Beloborodov, A.M., 2007. Neutrino-cooled Accretion Disks around Spinning Black Holes. *ApJ* 657, 383–399. doi:[10.1086/508923](https://doi.org/10.1086/508923), [arXiv:astro-ph/0607145](https://arxiv.org/abs/astro-ph/0607145).

- Di Matteo, T., Perna, R., Narayan, R., 2002. Neutrino Trapping and Accretion Models for Gamma-Ray Bursts. *ApJ* 579, 706–715. doi:[10.1086/342832](https://doi.org/10.1086/342832), [arXiv:astro-ph/0207319](https://arxiv.org/abs/astro-ph/0207319).
- Eichler, D., Livio, M., Piran, T., Schramm, D.N., 1989. Nucleosynthesis, neutrino bursts and γ -rays from coalescing neutron stars. *Nature* 340, 126–128. doi:[10.1038/340126a0](https://doi.org/10.1038/340126a0).
- Fishbone, L.G., Moncrief, V., 1976. Relativistic fluid disks in orbit around Kerr black holes. *ApJ* 207, 962–976. doi:[10.1086/154565](https://doi.org/10.1086/154565).
- Fryer, C.L., Woosley, S.E., Herant, M., Davies, M.B., 1999. Merging White Dwarf/Black Hole Binaries and Gamma-Ray Bursts. *ApJ* 520, 650–660. doi:[10.1086/307467](https://doi.org/10.1086/307467), [arXiv:astro-ph/9808094](https://arxiv.org/abs/astro-ph/9808094).
- Fu, S.Y., Xu, D., Lei, W.H., de Ugarte Postigo, A., Kann, D.A., Thöne, C.C., Agüí Fernández, J.F., Shuang-Xi, Y., Xie, W., Zou, Y.C., Liu, X., Jiang, S.Q., Lu, T.H., An, J., Zhu, Z.P., Zheng, J., Tang, Q.W., Zhao, P.W., Xin, L.P., Wei, J.Y., 2024. Unveiling the Multifaceted GRB 200613A: Prompt Emission Dynamics, Afterglow Evolution, and the Host Galaxy’s Properties. *ApJ* 974, 221. doi:[10.3847/1538-4357/ad6306](https://doi.org/10.3847/1538-4357/ad6306), [arXiv:2407.15824](https://arxiv.org/abs/2407.15824).
- Gammie, C.F., McKinney, J.C., Tóth, G., 2003. HARM: A Numerical Scheme for General Relativistic Magnetohydrodynamics. *ApJ* 589, 444–457. doi:[10.1086/374594](https://doi.org/10.1086/374594), [arXiv:astro-ph/0301509](https://arxiv.org/abs/astro-ph/0301509).
- Gao, H., Lei, W.H., Zhu, Z.P., 2022. GRB 211211A: a Prolonged Central Engine under a Strong Magnetic Field Environment. *ApJL* 934, L12. doi:[10.3847/2041-8213/ac80c7](https://doi.org/10.3847/2041-8213/ac80c7), [arXiv:2205.05031](https://arxiv.org/abs/2205.05031).
- Gao, H., Zhang, B., 2015. Photosphere Emission from a Hybrid Relativistic Outflow with Arbitrary Dimensionless Entropy and Magnetization in GRBs. *ApJ* 801, 103. doi:[10.1088/0004-637X/801/2/103](https://doi.org/10.1088/0004-637X/801/2/103), [arXiv:1409.3584](https://arxiv.org/abs/1409.3584).
- Gu, W.M., Liu, T., Lu, J.F., 2006. Neutrino-dominated Accretion Models for Gamma-Ray Bursts: Effects of General Relativity and Neutrino Opacity. *ApJL* 643, L87–L90. doi:[10.1086/505140](https://doi.org/10.1086/505140), [arXiv:astro-ph/0604370](https://arxiv.org/abs/astro-ph/0604370).
- Janiuk, A., 2017. Microphysics in the Gamma-Ray Burst Central Engine. *ApJ* 837, 39. doi:[10.3847/1538-4357/aa5f16](https://doi.org/10.3847/1538-4357/aa5f16), [arXiv:1609.09361](https://arxiv.org/abs/1609.09361).
- Janiuk, A., 2019. The r-process Nucleosynthesis in the Outflows from Short GRB Accretion Disks. *ApJ* 882, 163. doi:[10.3847/1538-4357/ab3349](https://doi.org/10.3847/1538-4357/ab3349), [arXiv:1907.00809](https://arxiv.org/abs/1907.00809).
- Janiuk, A., James, B., Palit, I., 2021. Variability of Magnetically Dominated Jets from Accreting Black Holes. *ApJ* 917, 102. doi:[10.3847/1538-4357/ac0624](https://doi.org/10.3847/1538-4357/ac0624), [arXiv:2105.13624](https://arxiv.org/abs/2105.13624).
- Janiuk, A., Mioduszewski, P., Moscibrodzka, M., 2013. Accretion and Outflow from a Magnetized, Neutrino Cooled Torus around the Gamma-Ray Burst Central Engine. *ApJ* 776, 105. doi:[10.1088/0004-637X/776/2/105](https://doi.org/10.1088/0004-637X/776/2/105), [arXiv:1308.4823](https://arxiv.org/abs/1308.4823).
- Janiuk, A., Sukova, P., Palit, I., 2018. Accretion in a Dynamical Spacetime and the Spinning Up of the Black Hole in the Gamma-Ray Burst Central Engine. *ApJ* 868, 68. doi:[10.3847/1538-4357/aae83f](https://doi.org/10.3847/1538-4357/aae83f), [arXiv:1810.05261](https://arxiv.org/abs/1810.05261).
- Janiuk, A., Yuan, Y., Perna, R., Di Matteo, T., 2007. Instabilities in the Time-Dependent Neutrino Disk in Gamma-Ray Bursts. *ApJ* 664, 1011–1025. doi:[10.1086/518761](https://doi.org/10.1086/518761), [arXiv:0704.1325](https://arxiv.org/abs/0704.1325).
- Kasliwal, M.M., Nakar, E., Singer, L.P., Kaplan, D.L., Cook, D.O., Van Sistine, A., Lau, R.M., Fremling, C., Gottlieb, O., Jencson, J.E., Adams, S.M., Feindt, U., Hotokezaka, K., Ghosh, S., Perley, D.A., Yu, P.C., Piran, T., Allison, J.R., Anupama, G.C., Balasubramanian, A., Bannister, K.W., Bally, J., Barnes, J., Barway, S., Bellm, E., Bhalerao, V., Bhattacharya, D., Blagorodnova, N., Bloom, J.S., Brady, P.R., Cannella, C., Chatterjee, D., Cenko, S.B., Cobb, B.E., Copperwheat, C., Corsi, A., De, K., Dobie, D., Emery, S.W.K., Evans, P.A., Fox, O.D., Frail, D.A., Frohmaier, C., Goobar, A., Hallinan, G., Harrison, F., Helou, G., Hinderer, T., Ho, A.Y.Q., Horesh, A., Ip, W.H., Itoh, R., Kasen, D., Kim, H., Kuin, N.P.M., Kupfer, T., Lynch, C., Madsen, K., Mazzali, P.A., Miller, A.A., Mooley, K., Murphy, T., Ngeow, C.C., Nichols, D., Nissanke, S., Nugent, P., Ofek, E.O., Qi, H., Quimby, R.M., Rosswog, S., Rusu, F., Sadler, E.M., Schmidt, P., Sollerman, J., Steele, I., Williamson, A.R., Xu, Y., Yan, L., Yatsu, Y., Zhang, C., Zhao, W., 2017. Illuminating gravitational waves: A concordant picture of photons from a neutron star merger. *Science* 358, 1559–1565. doi:[10.1126/science.aap9455](https://doi.org/10.1126/science.aap9455), [arXiv:1710.05436](https://arxiv.org/abs/1710.05436).
- Kathirgamaraju, A., Li, H., Ryan, B.R., Tchekhovskoy, A., 2024. Afterglows from Binary Neutron Star Post-

- merger Systems Embedded in Active Galactic Nuclei Disks. *ApJ* 972, 101. doi:[10.3847/1538-4357/ad63a3](https://doi.org/10.3847/1538-4357/ad63a3), [arXiv:2311.03571](https://arxiv.org/abs/2311.03571).
- Lee, H.K., Wijers, R.A.M.J., Brown, G.E., 2000. The Blandford-Znajek process as a central engine for a gamma-ray burst. *Phys. Rep.* 325, 83–114. doi:[10.1016/S0370-1573\(99\)00084-8](https://doi.org/10.1016/S0370-1573(99)00084-8), [arXiv:astro-ph/9906213](https://arxiv.org/abs/astro-ph/9906213).
- Lei, W.H., Wang, D.X., Ma, R.Y., 2005. A Toy Model for Gamma-Ray Bursts in Type Ib/c Supernovae. *ApJ* 619, 420–426. doi:[10.1086/426378](https://doi.org/10.1086/426378), [arXiv:astro-ph/0410219](https://arxiv.org/abs/astro-ph/0410219).
- Lei, W.H., Wang, D.X., Zhang, L., Gan, Z.M., Zou, Y.C., Xie, Y., 2009. Magnetically Torqued Neutrino-dominated Accretion Flows for Gamma-ray Bursts. *ApJ* 700, 1970–1976. doi:[10.1088/0004-637X/700/2/1970](https://doi.org/10.1088/0004-637X/700/2/1970), [arXiv:0906.1635](https://arxiv.org/abs/0906.1635).
- Lei, W.H., Zhang, B., 2011. Black Hole Spin in Sw J1644+57 and Sw J2058+05. *ApJL* 740, L27. doi:[10.1088/2041-8205/740/1/L27](https://doi.org/10.1088/2041-8205/740/1/L27), [arXiv:1108.3115](https://arxiv.org/abs/1108.3115).
- Lei, W.H., Zhang, B., Liang, E.W., 2013. Hyperaccreting Black Hole as Gamma-Ray Burst Central Engine. I. Baryon Loading in Gamma-Ray Burst Jets. *ApJ* 765, 125. doi:[10.1088/0004-637X/765/2/125](https://doi.org/10.1088/0004-637X/765/2/125), [arXiv:1209.4427](https://arxiv.org/abs/1209.4427).
- Lei, W.H., Zhang, B., Wu, X.F., Liang, E.W., 2017. Hyperaccreting Black Hole as Gamma-Ray Burst Central Engine. II. Temporal Evolution of the Central Engine Parameters during the Prompt and Afterglow Phases. *ApJ* 849, 47. doi:[10.3847/1538-4357/aa9074](https://doi.org/10.3847/1538-4357/aa9074), [arXiv:1708.05043](https://arxiv.org/abs/1708.05043).
- Li, L., Wu, X.F., Lei, W.H., Dai, Z.G., Liang, E.W., Ryde, F., 2018. Constraining the Type of Central Engine of GRBs with Swift Data. *ApJS* 236, 26. doi:[10.3847/1538-4365/aabaf3](https://doi.org/10.3847/1538-4365/aabaf3), [arXiv:1712.09390](https://arxiv.org/abs/1712.09390).
- Li, L.X., Paczyński, B., 2000. Extracting Energy from Accretion into a Kerr Black Hole. *ApJL* 534, L197–L198. doi:[10.1086/312678](https://doi.org/10.1086/312678), [arXiv:astro-ph/0003187](https://arxiv.org/abs/astro-ph/0003187).
- Liu, T., 2018. Black Hole Hyperaccretion and Gamma-ray Bursts. *Acta Astronomica Sinica* 59, 45.
- Liu, T., Gu, W.M., Xue, L., Lu, J.F., 2007. Structure and Luminosity of Neutrino-cooled Accretion Disks. *ApJ* 661, 1025–1033. doi:[10.1086/513689](https://doi.org/10.1086/513689), [arXiv:astro-ph/0702186](https://arxiv.org/abs/astro-ph/0702186).
- Liu, T., Gu, W.M., Zhang, B., 2017. Neutrino-dominated accretion flows as the central engine of gamma-ray bursts. *New Astron. Rev.* 79, 1–25. doi:[10.1016/j.newar.2017.07.001](https://doi.org/10.1016/j.newar.2017.07.001), [arXiv:1705.05516](https://arxiv.org/abs/1705.05516).
- Lloyd-Ronning, N., Lei, W.H., Xie, W., 2018. An MAD explanation for the correlation between bulk Lorentz factor and minimum variability time-scale. *MNRAS* 478, 3525–3529. doi:[10.1093/mnras/sty1030](https://doi.org/10.1093/mnras/sty1030), [arXiv:1804.04194](https://arxiv.org/abs/1804.04194).
- MacFadyen, A.I., Woosley, S.E., 1999. Collapsars: Gamma-Ray Bursts and Explosions in “Failed Supernovae”. *ApJ* 524, 262–289. doi:[10.1086/307790](https://doi.org/10.1086/307790), [arXiv:astro-ph/9810274](https://arxiv.org/abs/astro-ph/9810274).
- McKinney, J.C., 2005. Total and Jet Blandford-Znajek Power in the Presence of an Accretion Disk. *ApJL* 630, L5–L8. doi:[10.1086/468184](https://doi.org/10.1086/468184), [arXiv:astro-ph/0506367](https://arxiv.org/abs/astro-ph/0506367).
- Noble, S.C., Gammie, C.F., McKinney, J.C., Del Zanna, L., 2006. Primitive Variable Solvers for Conservative General Relativistic Magnetohydrodynamics. *ApJ* 641, 626–637. doi:[10.1086/500349](https://doi.org/10.1086/500349), [arXiv:astro-ph/0512420](https://arxiv.org/abs/astro-ph/0512420).
- Paczynski, B., 1991. On the galactic origin of gamma-ray bursts. *Acta Astron.* 41, 157–166.
- Paczyński, B., 1998. Are Gamma-Ray Bursts in Star-Forming Regions? *ApJL* 494, L45–L48. doi:[10.1086/311148](https://doi.org/10.1086/311148), [arXiv:astro-ph/9710086](https://arxiv.org/abs/astro-ph/9710086).
- Perna, R., Lazzati, D., Cantiello, M., 2021. Electromagnetic Signatures of Relativistic Explosions in the Disks of Active Galactic Nuclei. *ApJL* 906, L7. doi:[10.3847/2041-8213/abd319](https://doi.org/10.3847/2041-8213/abd319), [arXiv:2011.08873](https://arxiv.org/abs/2011.08873).
- Popham, R., Woosley, S.E., Fryer, C., 1999. Hyperaccreting Black Holes and Gamma-Ray Bursts. *ApJ* 518, 356–374. doi:[10.1086/307259](https://doi.org/10.1086/307259), [arXiv:astro-ph/9807028](https://arxiv.org/abs/astro-ph/9807028).
- Rosswog, S., Ramirez-Ruiz, E., Davies, M.B., 2003. High-resolution calculations of merging neutron stars - III. Gamma-ray bursts. *MNRAS* 345, 1077–1090. doi:[10.1046/j.1365-2966.2003.07032.x](https://doi.org/10.1046/j.1365-2966.2003.07032.x), [arXiv:astro-ph/0306418](https://arxiv.org/abs/astro-ph/0306418).

- Sapountzis, K., Janiuk, A., 2019. The MRI Imprint on the Short-GRB Jets. *ApJ* 873, 12. doi:[10.3847/1538-4357/ab0107](https://doi.org/10.3847/1538-4357/ab0107), [arXiv:1802.02786](https://arxiv.org/abs/1802.02786).
- Tchekhovskoy, A., McKinney, J.C., 2012. Prograde and retrograde black holes: whose jet is more powerful? *MNRAS* 423, L55–L59. doi:[10.1111/j.1745-3933.2012.01256.x](https://doi.org/10.1111/j.1745-3933.2012.01256.x), [arXiv:1201.4385](https://arxiv.org/abs/1201.4385).
- Tchekhovskoy, A., Narayan, R., McKinney, J.C., 2010. Black Hole Spin and The Radio Loud/Quiet Dichotomy of Active Galactic Nuclei. *ApJ* 711, 50–63. doi:[10.1088/0004-637X/711/1/50](https://doi.org/10.1088/0004-637X/711/1/50), [arXiv:0911.2228](https://arxiv.org/abs/0911.2228).
- Wang, D.X., Xiao, K., Lei, W.H., 2002. Evolution characteristics of the central black hole of a magnetized accretion disc. *MNRAS* 335, 655–664. doi:[10.1046/j.1365-8711.2002.05652.x](https://doi.org/10.1046/j.1365-8711.2002.05652.x), [arXiv:astro-ph/0209368](https://arxiv.org/abs/astro-ph/0209368).
- Woosley, S.E., 1993. Gamma-Ray Bursts from Stellar Mass Accretion Disks around Black Holes. *ApJ* 405, 273. doi:[10.1086/172359](https://doi.org/10.1086/172359).
- Xie, W., Lei, W.H., Wang, D.X., 2016. Numerical and Analytical Solutions of Neutrino-dominated Accretion Flows with a Non-zero Torque Boundary Condition and its Applications in Gamma-Ray Bursts. *ApJ* 833, 129. doi:[10.3847/1538-4357/833/2/129](https://doi.org/10.3847/1538-4357/833/2/129), [arXiv:1609.09183](https://arxiv.org/abs/1609.09183).
- Xie, W., Lei, W.H., Wang, D.X., 2017. What Can We Learn about GRB from the Variability Timescale Related Correlations? *ApJ* 838, 143. doi:[10.3847/1538-4357/aa6718](https://doi.org/10.3847/1538-4357/aa6718), [arXiv:1703.04863](https://arxiv.org/abs/1703.04863).
- Yi, S.X., Lei, W.H., Zhang, B., Dai, Z.G., Wu, X.F., Liang, E.W., 2017. Lorentz factor - Beaming corrected energy/luminosity correlations and GRB central engine models. *Journal of High Energy Astrophysics* 13, 1–9. doi:[10.1016/j.jheap.2017.01.001](https://doi.org/10.1016/j.jheap.2017.01.001), [arXiv:1612.06586](https://arxiv.org/abs/1612.06586).
- Yi, S.X., Xie, W., Ma, S.B., Lei, W.H., Du, M., 2021. Constraining properties of GRB central engines with X-ray flares. *MNRAS* 507, 1047–1054. doi:[10.1093/mnras/stab2186](https://doi.org/10.1093/mnras/stab2186), [arXiv:2107.12538](https://arxiv.org/abs/2107.12538).
- Yuan, C., Murase, K., Guetta, D., Pe’er, A., Bartos, I., Mészáros, P., 2022. GeV Signatures of Short Gamma-Ray Bursts in Active Galactic Nuclei. *ApJ* 932, 80. doi:[10.3847/1538-4357/ac6ddf](https://doi.org/10.3847/1538-4357/ac6ddf), [arXiv:2112.07653](https://arxiv.org/abs/2112.07653).
- Yuan, H.Y., Lei, W.H., 2025. The Multiband Emission of the Two-component Gamma-Ray Burst Jet Influenced by Progenitor Winds within the Accretion Disk of Active Galactic Nuclei. *ApJ* 987, 167. doi:[10.3847/1538-4357/addbe4](https://doi.org/10.3847/1538-4357/addbe4), [arXiv:2408.06593](https://arxiv.org/abs/2408.06593).
- Yuan, Y.F., 2005. Electron-positron capture rates and a steady state equilibrium condition for an electron-positron plasma with nucleons. *Phys. Rev. D* 72, 013007. doi:[10.1103/PhysRevD.72.013007](https://doi.org/10.1103/PhysRevD.72.013007), [arXiv:astro-ph/0507311](https://arxiv.org/abs/astro-ph/0507311).
- Zhang, B., Wang, X.Y., Zheng, J.H., 2024. The BOAT GRB 221009A: A Poynting-flux-dominated narrow jet surrounded by a matter-dominated structured jet wing. *Journal of High Energy Astrophysics* 41, 42–53. doi:[10.1016/j.jheap.2024.01.002](https://doi.org/10.1016/j.jheap.2024.01.002), [arXiv:2311.14180](https://arxiv.org/abs/2311.14180).
- Zhang, B.B., Zhang, B., Castro-Tirado, A.J., Dai, Z.G., Tam, P.H.T., Wang, X.Y., Hu, Y.D., Karpov, S., Pozanenko, A., Zhang, F.W., Mazaeva, E., Minaev, P., Volnova, A., Oates, S., Gao, H., Wu, X.F., Shao, L., Tang, Q.W., Beskin, G., Biryukov, A., Bondar, S., Ivanov, E., Katkova, E., Orekhova, N., Perkov, A., Sasyuk, V., Mankiewicz, L., Żarnecki, A.F., Cwiek, A., Opiela, R., Zadrożny, A., Aptekar, R., Frederiks, D., Svinkin, D., Kusakina, A., Inasaridze, R., Burhonov, O., Romyantsev, V., Klunko, E., Moskvitin, A., Fatkhullin, T., Sokolov, V.V., Valeev, A.F., Jeong, S., Park, I.H., Caballero-García, M.D., Cunniffe, R., Tello, J.C., Ferrero, P., Pandey, S.B., Jelínek, M., Peng, F.K., Sánchez-Ramírez, R., Castellón, A., 2018. Transition from fireball to Poynting-flux-dominated outflow in the three-episode GRB 160625B. *Nature Astronomy* 2, 69–75. doi:[10.1038/s41550-017-0309-8](https://doi.org/10.1038/s41550-017-0309-8), [arXiv:1612.03089](https://arxiv.org/abs/1612.03089).
- Zhu, J.P., Zhang, B., Yu, Y.W., Gao, H., 2021. Neutron Star Mergers in Active Galactic Nucleus Accretion Disks: Cocoon and Ejecta Shock Breakouts. *ApJL* 906, L11. doi:[10.3847/2041-8213/abd412](https://doi.org/10.3847/2041-8213/abd412), [arXiv:2011.08428](https://arxiv.org/abs/2011.08428).